



PARA - PArameterization informed by RAdar - Update

T. Scharbach^{1,2}, S. Trömel¹

¹ Institute for Geosciences, Department Meteorology, University of Bonn, 53121, Germany;

² toscha@uni-bonn.de



photo of Bonn X-band radar by V. Pejic

Creation of a stratiform climatology of different ice-microphysical retrievals (IWC, N_t and D_m) and polarimetric variables using large BoXPol dataset

- Comparisons of BoXPol statistics with profiles of ICON runs using EMVORADO as observation operator [Blahak, 2016]

Creation of a stratiform climatology of different ice-microphysical retrievals (IWC, N_t and D_m) and polarimetric variables using large BoXPol dataset

- Comparisons of BoXPol statistics with profiles of ICON runs using EMVORADO as observation operator [Blahak, 2016]
 - comparison with simulations can reveal inadequate parameterisations and/or approximations

Creation of a stratiform climatology of different ice-microphysical retrievals (IWC, N_t and D_m) and polarimetric variables using large BoXPol dataset

- Comparisons of BoXPol statistics with profiles of ICON runs using EMVORADO as observation operator [Blahak, 2016]
 - comparison with simulations can reveal inadequate parameterisations and/or approximations
- Improvement for filtering of stratiform sequences via a new robust and automated algorithm →

Motivation and Objectives

Creation of a stratiform climatology of different ice-microphysical retrievals (IWC, N_t and D_m) and polarimetric variables using large BoXPol dataset

- Comparisons of BoXPol statistics with profiles of ICON runs using EMVORADO as observation operator [Blahak, 2016]

→ comparison with simulations can reveal inadequate parameterisations and/or approximations

- Improvement for filtering of stratiform sequences via a new robust and automated algorithm →

Shannon information entropy [Shannon, 1948] in combination with ML detection [Wolfensberger et al., 2016]

Creation of a stratiform climatology of different ice-microphysical retrievals (IWC, N_t and D_m) and polarimetric variables using large BoXPol dataset

- Comparisons of BoXPol statistics with profiles of ICON runs using EMVORADO as observation operator [Blahak, 2016]
→ comparison with simulations can reveal inadequate parameterisations and/or approximations
- Improvement for filtering of stratiform sequences via a new robust and automated algorithm →
Shannon information entropy [Shannon, 1948] in combination with ML detection [Wolfensberger et al., 2016]

Creation of a stratiform climatology of different ice-microphysical retrievals (IWC, N_t and D_m) and polarimetric variables using large BoXPol dataset

- Comparisons of BoXPol statistics with profiles of ICON runs using EMVORADO as observation operator [Blahak, 2016]
→ comparison with simulations can reveal inadequate parameterisations and/or approximations
- Improvement for filtering of stratiform sequences via a new robust and automated algorithm →
Shannon information entropy [Shannon, 1948] in combination with ML detection [Wolfensberger et al., 2016]

Filtering method

- ML detection applied to QVPs, with estimation of an average K_{DP} within the ML [Trömel et al., 2019]
- Timesteps without detected ML are directly classified as convective

Filtering method

- ML detection applied to QVPs, with estimation of an average K_{DP} within the ML [Trömel et al., 2019]
- Timesteps without detected ML are directly classified as convective
- Homogeneous conditions for successful reduction of statistical errors and stratiform conditions

Filtering method

- ML detection applied to QVPs, with estimation of an average K_{DP} within the ML [Trömel et al., 2019]
- Timesteps without detected ML are directly classified as convective
- Homogeneous conditions for successful reduction of statistical errors and stratiform conditions
- Usage of a normalized version of shannon information Entropy in the range from (0 – 1)

Filtering method

- ML detection applied to QVPs, with estimation of an average K_{DP} within the ML [Trömel et al., 2019]
- Timesteps without detected ML are directly classified as convective
- Homogeneous conditions for successful reduction of statistical errors and stratiform conditions
- Usage of a normalized version of shannon information Entropy in the range from (0 – 1)
 - 0: Total heterogeneous conditions
 - 1: Fully homogeneous conditions

Filtering method

- ML detection applied to QVPs, with estimation of an average K_{DP} within the ML [Trömel et al., 2019]
- Timesteps without detected ML are directly classified as convective
- Homogeneous conditions for successful reduction of statistical errors and stratiform conditions
- Usage of a normalized version of shannon information Entropy in the range from (0 – 1)
 - 0: Total heterogeneous conditions
 - 1: Fully homogeneous conditions

→ calculated over K_{DP} , ρ_{HV} and Z_{DR} , Z_H in linear scale with subsequent using the minimum value

Filtering method

- ML detection applied to QVPs, with estimation of an average K_{DP} within the ML [Trömel et al., 2019]
- Timesteps without detected ML are directly classified as convective
- Homogeneous conditions for successful reduction of statistical errors and stratiform conditions
- Usage of a normalized version of shannon information Entropy in the range from (0 – 1)
 - 0: Total heterogeneous conditions
 - 1: Fully homogeneous conditions
 - calculated over K_{DP} , ρ_{HV} and Z_{DR} , Z_H in linear scale with subsequent using the minimum value
 - used entropy threshold of ≥ 0.8 for creating stratiform statistics

Filtering method

- ML detection applied to QVPs, with estimation of an average K_{DP} within the ML [Trömel et al., 2019]
- Timesteps without detected ML are directly classified as convective
- Homogeneous conditions for successful reduction of statistical errors and stratiform conditions
- Usage of a normalized version of shannon information Entropy in the range from (0 – 1)
 - 0: Total heterogeneous conditions
 - 1: Fully homogeneous conditions
 - calculated over K_{DP} , ρ_{HV} and Z_{DR} , Z_H in linear scale with subsequent using the minimum value
 - used entropy threshold of ≥ 0.8 for creating stratiform statistics

Filtering method example

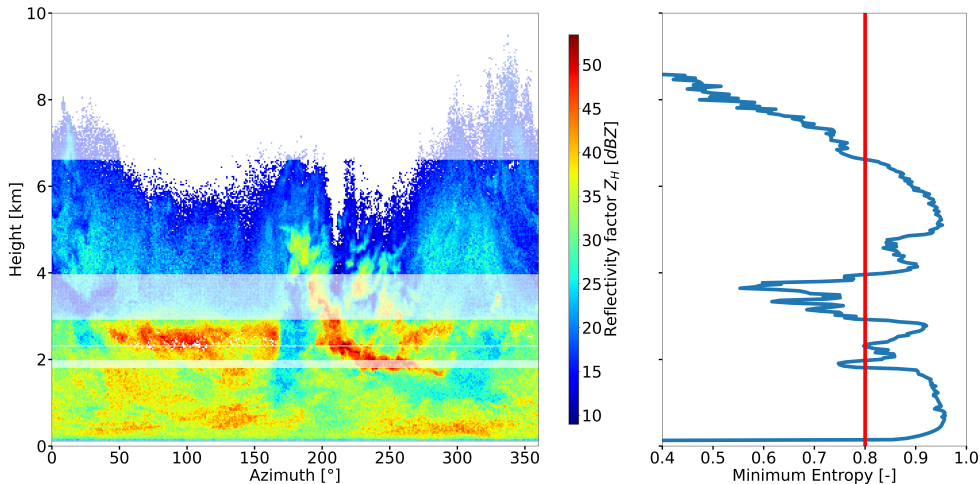


Figure 1: Horizontal reflectivity Z_H (left) monitored with BoXPOL on 30 May 2016 at 03:06 UTC together with the profile of calculated minimum normalised Shannon information entropy (right). The applied threshold is indicated as red line and the excluded sequences displayed as transparent regions.

- Filtering approach applied to synthetic and observation data:
 - 1168.5 hours of BoXPol observations from 627 different days (2014-2018)
 - 109.2 hours from 11 different days (2017-2018) for JuXPol + BoXPol synthetic data
- To increase statistical significance, ICON simulations of IWC, D_m and N_t of JuXPol + BoXPol in retrieval space are merged with all simulated C-band stations from DWD

Used ice-microphysical retrievals and simulated counterparts

$$D_m(K_{DP}, Z_{dp}, Z_h) = \begin{cases} D_m(K_{DP}, Z_{dp}) & \text{if } Z_{DR} \geq 0.4 \text{ dB} \\ D_m(K_{DP}, Z_h) & \text{if } Z_{DR} < 0.4 \text{ dB} \end{cases} \quad (1)$$

$$\text{IWC}(K_{DP}, Z_{dr}, Z_h) = \begin{cases} \text{IWC}(K_{DP}, Z_{dr}) & \text{if } Z_{DR} \geq 0.4 \text{ dB} \\ \text{IWC}(K_{DP}, Z_h) & \text{if } Z_{DR} < 0.4 \text{ dB} \end{cases} \quad (2)$$

$$N_t = N_t(\text{IWC}(K_{DP}, Z_{dr}, Z_h)) \quad (3)$$

following [Bukovčić et al., 2020], [Bukovčić et al., 2018], [Ryzhkov and Zrnica, 2019] and [Carlin et al., 2021]

- Simulated N_t is the sum of all number densities [$1/m^3$]

Used ice-microphysical retrievals and simulated counterparts

$$D_m(K_{DP}, Z_{dp}, Z_h) = \begin{cases} D_m(K_{DP}, Z_{dp}) & \text{if } Z_{DR} \geq 0.4 \text{ dB} \\ D_m(K_{DP}, Z_h) & \text{if } Z_{DR} < 0.4 \text{ dB} \end{cases} \quad (1)$$

$$\text{IWC}(K_{DP}, Z_{dr}, Z_h) = \begin{cases} \text{IWC}(K_{DP}, Z_{dr}) & \text{if } Z_{DR} \geq 0.4 \text{ dB} \\ \text{IWC}(K_{DP}, Z_h) & \text{if } Z_{DR} < 0.4 \text{ dB} \end{cases} \quad (2)$$

$$N_t = N_t(\text{IWC}(K_{DP}, Z_{dr}, Z_h)) \quad (3)$$

following [Bukovčić et al., 2020], [Bukovčić et al., 2018], [Ryzhkov and Zrnica, 2019] and [Carlin et al., 2021]

- Simulated N_t is the sum of all number densities [$1/m^3$]
- Simulated IWC is the sum of the densities of all ice hydrometeor classes [g/m^3]

Used ice-microphysical retrievals and simulated counterparts

$$D_m(K_{DP}, Z_{dp}, Z_h) = \begin{cases} D_m(K_{DP}, Z_{dp}) & \text{if } Z_{DR} \geq 0.4 \text{ dB} \\ D_m(K_{DP}, Z_h) & \text{if } Z_{DR} < 0.4 \text{ dB} \end{cases} \quad (1)$$

$$\text{IWC}(K_{DP}, Z_{dr}, Z_h) = \begin{cases} \text{IWC}(K_{DP}, Z_{dr}) & \text{if } Z_{DR} \geq 0.4 \text{ dB} \\ \text{IWC}(K_{DP}, Z_h) & \text{if } Z_{DR} < 0.4 \text{ dB} \end{cases} \quad (2)$$

$$N_t = N_t(\text{IWC}(K_{DP}, Z_{dr}, Z_h)) \quad (3)$$

following [Bukovčić et al., 2020], [Bukovčić et al., 2018], [Ryzhkov and Zrnica, 2019] and [Carlin et al., 2021]

- Simulated N_t is the sum of all number densities [$1/m^3$]
- Simulated IWC is the sum of the densities of all ice hydrometer classes [g/m^3]
- and D_m is the ratio of the fourth to the third PSD moment, estimated with the densities of all ice hydrometer classes

Used ice-microphysical retrievals and simulated counterparts

$$D_m(K_{DP}, Z_{dp}, Z_h) = \begin{cases} D_m(K_{DP}, Z_{dp}) & \text{if } Z_{DR} \geq 0.4 \text{ dB} \\ D_m(K_{DP}, Z_h) & \text{if } Z_{DR} < 0.4 \text{ dB} \end{cases} \quad (1)$$

$$\text{IWC}(K_{DP}, Z_{dr}, Z_h) = \begin{cases} \text{IWC}(K_{DP}, Z_{dr}) & \text{if } Z_{DR} \geq 0.4 \text{ dB} \\ \text{IWC}(K_{DP}, Z_h) & \text{if } Z_{DR} < 0.4 \text{ dB} \end{cases} \quad (2)$$

$$N_t = N_t(\text{IWC}(K_{DP}, Z_{dr}, Z_h)) \quad (3)$$

following [Bukovčić et al., 2020], [Bukovčić et al., 2018], [Ryzhkov and Zrnica, 2019] and [Carlin et al., 2021]

- Simulated N_t is the sum of all number densities [$1/m^3$]
- Simulated IWC is the sum of the densities of all ice hydrometer classes [g/m^3]
- and D_m is the ratio of the fourth to the third PSD moment, estimated with the densities of all ice hydrometer classes

CFTD of retrieved D_m and simulated D_m

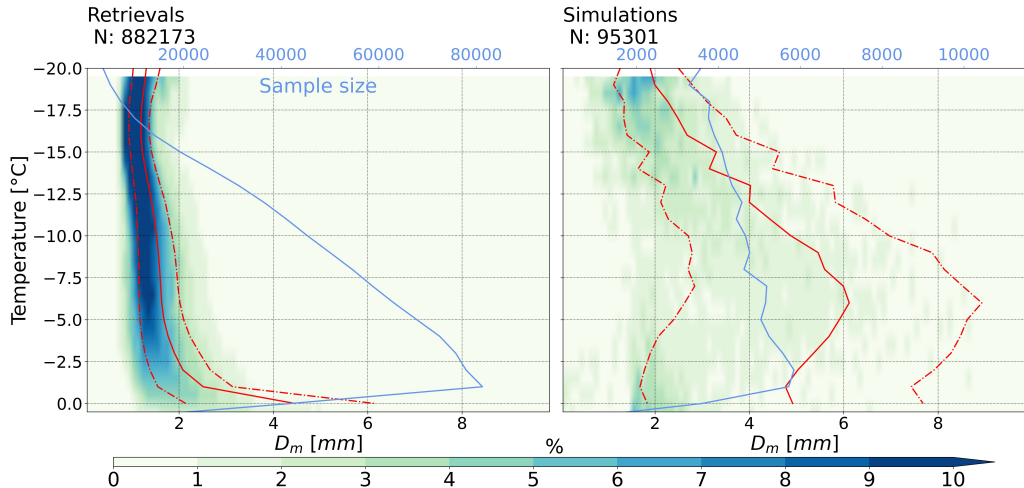


Figure 2: CFTDs of retrieved D_m (left) and simulated D_m (right), with The solid red line representing the mean and the dashed red lines the 20th and 80th percentiles. The blue line shows the number of samples in a 1 °C layer. Temperature information is taken from ERA5 [Hersbach et al., 2020] and ICON.

CFTD of retrieved N_t and simulated N_t

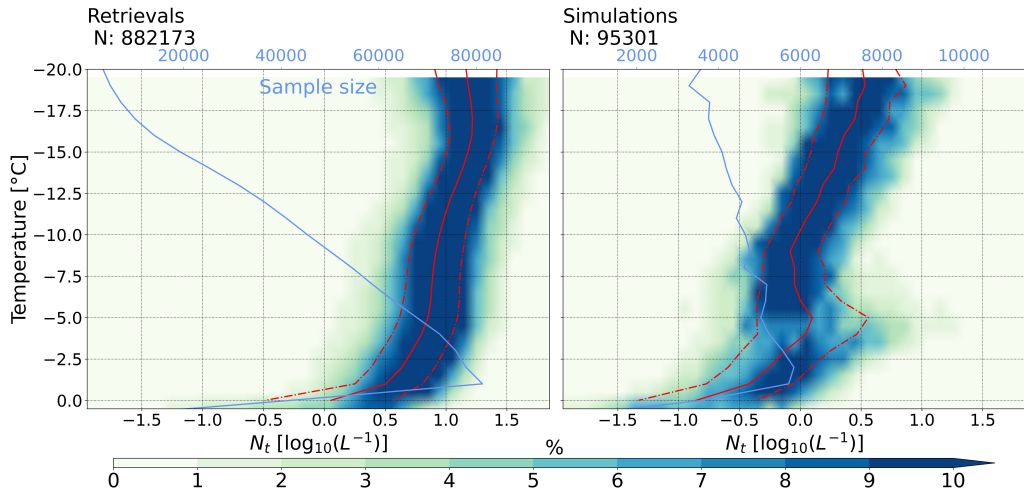


Figure 3: CFTDs of retrieved N_t (left) and simulated N_t (right), with The solid red line representing the mean and the dashed red lines the 20th and 80th percentiles. The blue line shows the number of samples in a 1 °C layer. Temperature information is taken from ERA5 [Hersbach et al., 2020] and ICON.

CFTD of retrieved IWC and simulated IWC

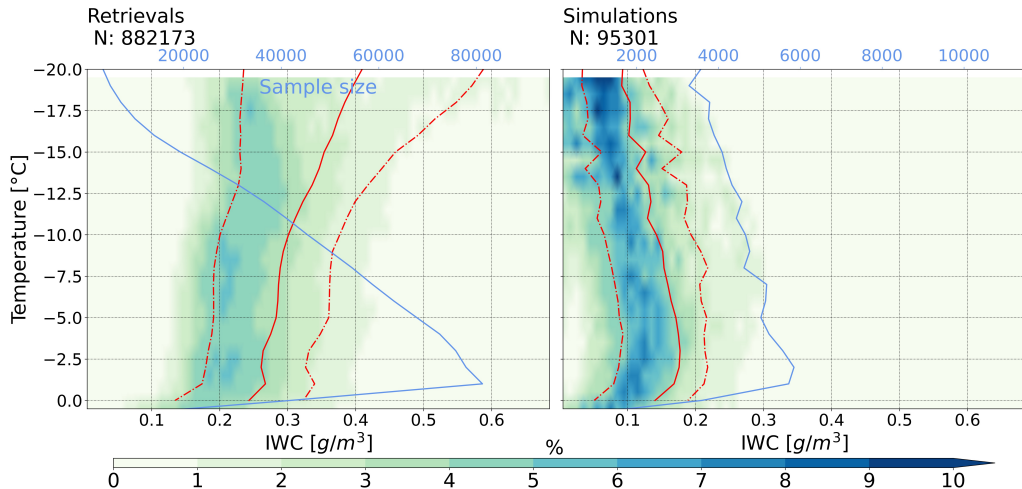


Figure 4: CFTDs of retrieved IWC (left) and simulated IWC (right), with The solid red line representing the mean and the dashed red lines the 20th and 80th percentiles. The blue line shows the number of samples in a 1 °C layer. Temperature information is taken from ERA5 [Hersbach et al., 2020] and ICON.

CFTD of observed Z_H and synthetic Z_H

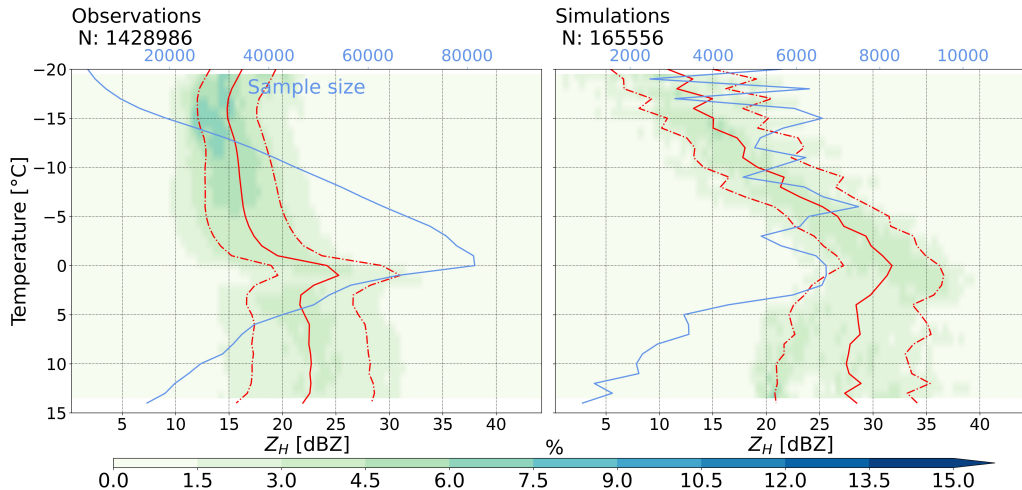


Figure 5: CFTDs of observed Z_H (left) and synthetic Z_H (right), with The solid red line representing the mean and the dashed red lines the 20th and 80th percentiles. The blue line shows the number of samples in a 1 °C layer. Temperature information is taken from ERA5 [Hersbach et al., 2020] and ICON.

CFTD of observed Z_{DR} and synthetic Z_{DR}

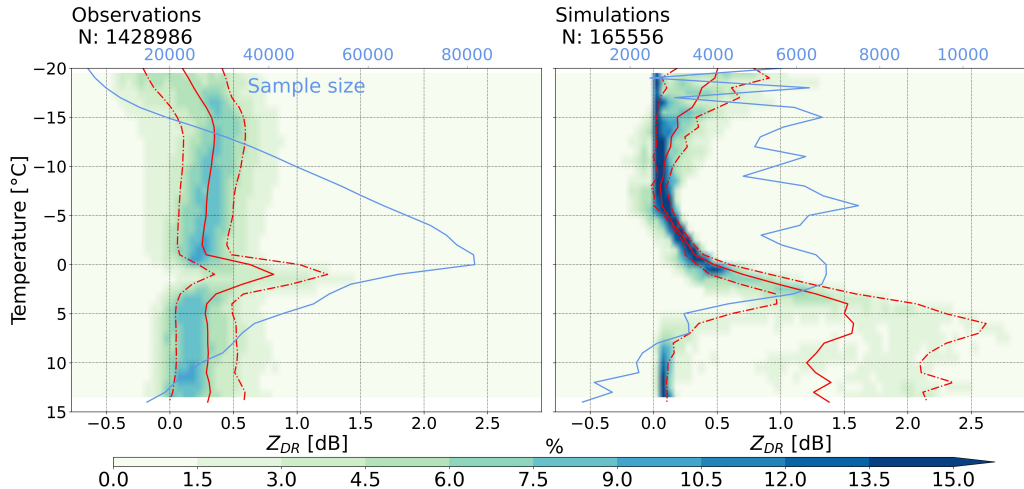


Figure 6: CFTDs of observed Z_{DR} (left) and synthetic Z_{DR} (right), with The solid red line representing the mean and the dashed red lines the 20th and 80th percentiles. The blue line shows the number of samples in a 1°C layer. Temperature information is taken from ERA5 [Hersbach et al., 2020] and ICON.

CFTD of observed K_{DP} and synthetic K_{DP}

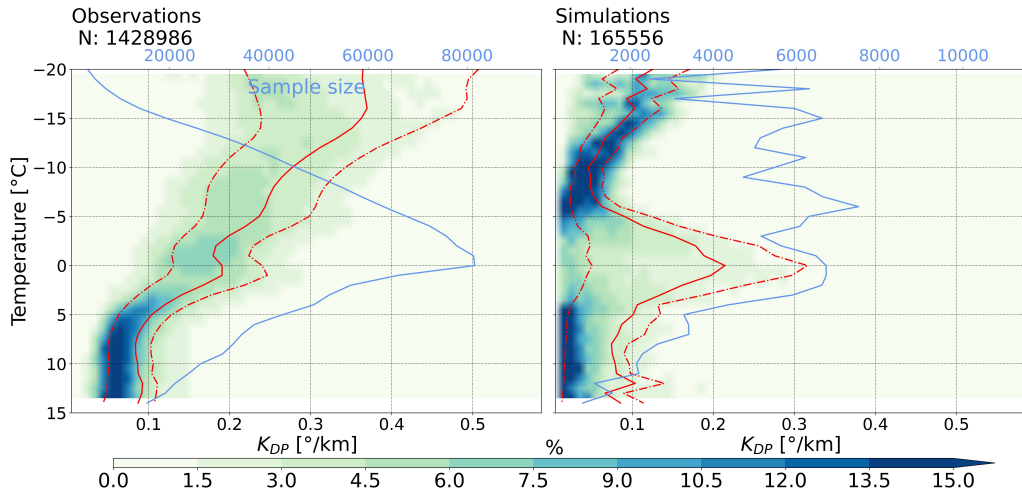


Figure 7: CFTDs of observed K_{DP} (left) and synthetic K_{DP} (right), with The solid red line representing the mean and the dashed red lines the 20th and 80th percentiles. The blue line shows the number of samples in a 1 °C layer. Temperature information is taken from ERA5 [Hersbach et al., 2020].

CFTD of observed ρ_{HV} and synthetic ρ_{HV}

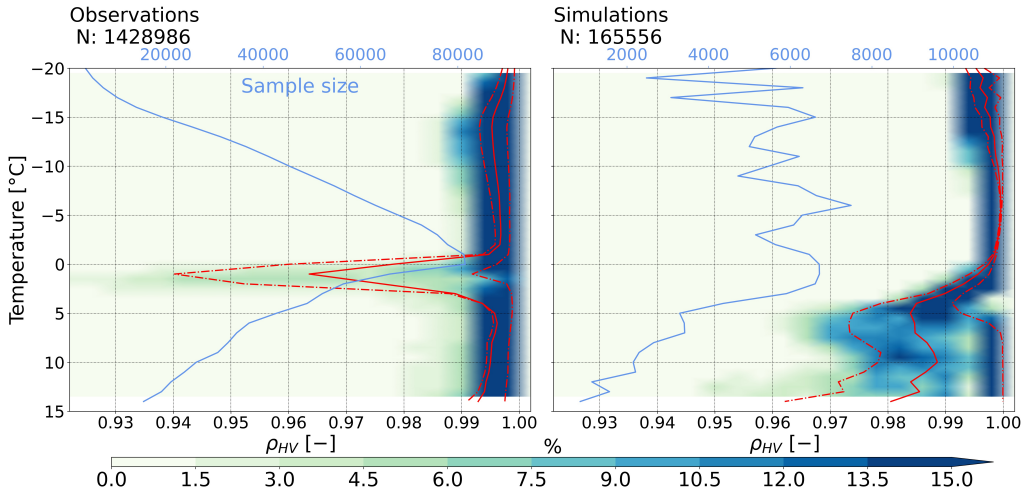


Figure 8: CFTDs of observed ρ_{HV} (left) and synthetic ρ_{HV} (right), with The solid red line representing the mean and the dashed red lines the 20th and 80th percentiles. The blue line shows the number of samples in a 1 °C layer. Temperature information is taken from ERA5 [Hersbach et al., 2020] and ICON.

Conclusions

- Shannon information entropy + ML detection as Filtering technique is very convenient to check events for stratiform conditions
- The detection of systematic differences between ice-microphysical retrievals (IWC , N_t , D_m) and ICON (density based) simulations, as well as polarimetric variables and their synthetic counterparts, reveals several discrepancies:

Conclusions

- Shannon information entropy + ML detection as Filtering technique is very convenient to check events for stratiform conditions
- The detection of systematic differences between ice-microphysical retrievals (IWC, N_t , D_m) and ICON (density based) simulations, as well as polarimetric variables and their synthetic counterparts, reveals several discrepancies:
 - 1) Generally there is a too small total number of ice particles (very low N_t)

Conclusions

- Shannon information entropy + ML detection as Filtering technique is very convenient to check events for stratiform conditions
- The detection of systematic differences between ice-microphysical retrievals (IWC, N_t , D_m) and ICON (density based) simulations, as well as polarimetric variables and their synthetic counterparts, reveals several discrepancies:
 - 1) Generally there is a too small total number of ice particles (very low N_t)
 - 2) This few particles generally experience too much aggregation (high D_m and strong gradient of Z_H aloft), with accompanied unrealistic high fall velocities towards warmer temperatures

Conclusions

- Shannon information entropy + ML detection as Filtering technique is very convenient to check events for stratiform conditions
- The detection of systematic differences between ice-microphysical retrievals (IWC, N_t , D_m) and ICON (density based) simulations, as well as polarimetric variables and their synthetic counterparts, reveals several discrepancies:
 - 1) Generally there is a too small total number of ice particles (very low N_t)
 - 2) This few particles generally experience too much aggregation (high D_m and strong gradient of Z_H aloft), with accompanied unrealistic high fall velocities towards warmer temperatures
 - 3) Strange inverse gradient of the simulated IWC compared to the retrieved IWC, with also generally too small values in the simulations

Conclusions

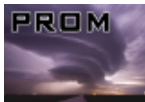
- Shannon information entropy + ML detection as Filtering technique is very convenient to check events for stratiform conditions
- The detection of systematic differences between ice-microphysical retrievals (IWC, N_t , D_m) and ICON (density based) simulations, as well as polarimetric variables and their synthetic counterparts, reveals several discrepancies:
 - 1) Generally there is a too small total number of ice particles (very low N_t)
 - 2) This few particles generally experience too much aggregation (high D_m and strong gradient of Z_H aloft), with accompanied unrealistic high fall velocities towards warmer temperatures
 - 3) Strange inverse gradient of the simulated IWC compared to the retrieved IWC, with also generally too small values in the simulations
→ needs further investigation regarding the complex interplay between different microphysical processes

Conclusions

- Shannon information entropy + ML detection as Filtering technique is very convenient to check events for stratiform conditions
- The detection of systematic differences between ice-microphysical retrievals (IWC, N_t , D_m) and ICON (density based) simulations, as well as polarimetric variables and their synthetic counterparts, reveals several discrepancies:
 - 1) Generally there is a too small total number of ice particles (very low N_t)
 - 2) This few particles generally experience too much aggregation (high D_m and strong gradient of Z_H aloft), with accompanied unrealistic high fall velocities towards warmer temperatures
 - 3) Strange inverse gradient of the simulated IWC compared to the retrieved IWC, with also generally too small values in the simulations
→ needs further investigation regarding the complex interplay between different microphysical processes

- 4) Beside too strong aggregation (near 0 dB in Z_{DR} and < 0.1 °/km in K_{DP} at around -7 °C) incorrectly assumed onset of wet graupel in EMVORADO, cause a sudden rapidly increase of Z_{DR} and K_{DP} towards warmer temperatures
- 5) The inadequate representation of the shape diversity in EMVORADO causes synthetic ρ_{HV} approach generally too high values, except the too low values due to the melting graupel below the ML

- 4) Beside too strong aggregation (near 0 dB in Z_{DR} and < 0.1 °/km in K_{DP} at around -7 °C) incorrectly assumed onset of wet graupel in EMVORADO, cause a sudden rapidly increase of Z_{DR} and K_{DP} towards warmer temperatures
- 5) The inadequate representation of the shape diversity in EMVORADO causes synthetic ρ_{HV} approach generally too high values, except the too low values due to the melting graupel below the ML









PARA - PArAmeterization informed by RAdar - Update




T. Scharbach^{1,2}, S. Trömel¹

¹ Institute for Geosciences, Department Meteorology, University of Bonn, 53121, Germany;

² toscha@uni-bonn.de

-  Blahak, U. (2016).
RADAR_MIE_LM and RADAR_MIELIB — calculation of radar reflectivity from model output.
Technical Report 28, Consortium for Small Scale Modeling (COSMO).
-  Bukovčić, P., Ryzhkov, A., and Zrnić, D. (2020).
Polarimetric relations for snow estimation—radar verification.
Journal of Applied Meteorology and Climatology, 59(5):991–1009.
-  Bukovčić, P., Ryzhkov, A., Zrnić, D., and Zhang, G. (2018).
Polarimetric radar relations for quantification of snow based on disdrometer data.
Journal of Applied Meteorology and Climatology, 57(1):103–120.

-  Carlin, J. T., Reeves, H. D., and Ryzhkov, A. V. (2021).
Polarimetric observations and simulations of sublimating snow: Implications for nowcasting.
Journal of Applied Meteorology and Climatology, 60(8):1035–1054.
-  Hersbach, H., Bell, B., Berrisford, P., Hirahara, S., Horányi, A., Muñoz-Sabater, J., Nicolas, J., Peubey, C., Radu, R., Schepers, D., et al. (2020).
The era5 global reanalysis.
Quarterly Journal of the Royal Meteorological Society, 146(730):1999–2049.
-  Ryzhkov, A. V. and Zrnica, D. S. (2019).
Radar polarimetry for weather observations.
Springer.

-  Shannon, C. E. (1948).
A mathematical theory of communication.
27(3):379–423.
-  Trömel, S., Ryzhkov, A. V., Hickman, B., Mühlbauer, K., and Simmer, C. (2019).
Polarimetric radar variables in the layers of melting and dendritic growth at x band—implications for a nowcasting strategy in stratiform rain.
Journal of Applied Meteorology and Climatology, 58(11):2497–2522.
-  Wolfensberger, D., Scipion, D., and Berne, A. (2016).
Detection and characterization of the melting layer based on polarimetric radar scans.
Quarterly Journal of the Royal Meteorological Society, 142:108–124.